Anal Bioanal Chem (2015) 407:447–453
DOI 10.1007/s00216-014-8290-x

RESEARCH PAPER

An ultrasensitive electrochemiluminescent biosensor for the detection of concanavalin A based on poly(ethylenimine) reduced graphene oxide and hollow gold nanoparticles

Juanjuan Zhang · Shihong Chen · Yuan Ruo · Xia Zhong · Xiaoping Wu

Received: 12 July 2014 / Revised: 31 August 2014 / Accepted: 22 October 2014 / Published online: 30 November 2014

Abstract A highly sensitive electrochemiluminescent (ECL) biosensor was designed for the detection of concanavalin A (ConA) based on glucose oxidase (GOx) as a recognition element by carbohydrate–lectin biospecific interaction, and poly(ethylenimine) (PEI) reduced graphene and hollow gold nanoparticles (HAuNPs) as supporting matrix and signal amplifier. The modification process and detection principle of the biosensor are briefly described as follows. First, PEI reduced graphene oxide with abundant amino groups was cast onto the surface of glassy carbon electrode to adsorb HAuNPs for improving the signal intensity in luminol/H_2O_2 ECL system. Next, GOx was further assembled onto the electrode by the interaction between Au and $–NH_2$. In the presence of glucose in the detection solution, GOx catalyzed glucose to generate H_2O_2 in situ, which served as a co-reactant of luminol to enhance ECL signal of luminol. Based on the fact that ConA could result in a decrease in ECL signal when immobilized on the electrode, an ECL biosensor was prepared for the determination of ConA. The ECL signal intensity was linear with the logarithm of ConA concentration and the linear range was from 1.0 to 20 ng/mL with a low detection limit of 0.31 ng/mL (signal to noise ratio =3). This strategy led to a nearly 1000-fold improvement in detection limit for ConA assays compared with previously reported method, thus exhibiting a great potential application in sensitive bioassays of ConA.

Keywords Biosensors · Electrochemiluminescence · Concanavalin A · Graphene · Hollow gold nanoparticles

Introduction

Molecular recognition between carbohydrates and specific proteins mediates many important physiological and pathophysiological processes, such as bacterial and viral infections, cellular growth and adhesion, cancer metastasis, inflammation, and immune surveillance [1]. Investigation of such interactions is significant for understanding basic biological processes and for the development of sensors [2]. Lectin, a carbohydrate-binding protein, is usually found in plants, animals, or microorganisms. One of them, concanavalin A (ConA), can specifically bind to some sugar groups such as mannose, dextran, and some glyco-proteins (glucose oxidase and HRP) by carbohydrate–lectin interactions [3, 4]. Recently, ConA was chosen as a lectin model for further study of molecular recognition in major researches [1, 2].

The reported detection methods for ConA mainly included optic analysis methods such as fluorescence spectroscopy, UV-visible spectroscopy, surface plasmon resonance, and electrochemical analysis methods such as differential pulse voltammetry and electrochemical impedance spectroscopy [1, 2, 5–11]. For example, fluorescent carbohydrate-protected Au nanodots were synthesized for detecting ConA [6]. Guo et al. [7] observed that the absorption of UV-vis spectrophotometry spectrum shifted when ConA was bound to the sugar residues of glycolipids immobilized onto nanogold slides, while almost no spectrum change was observed when another nonspecific protein molecule met the nanogold slides. Based on this observation, a sensitive gold nanoparticles-based biosensor was designed for ConA determination. Loaiza et al. [1] described the development of nanostructured impedimetric

Electronic supplementary material The online version of this article (doi:10.1007/s00216-014-8290-x) contains supplementary material, which is available to authorized users.

J. Zhang · S. Chen (✉) · Y. Ruo · X. Zhong · X. Wu
Key Laboratory of Luminescent and Real-Time Analytical Chemistry, Ministry of Education, College of Chemistry and Chemical Engineering, Southwest University, Chongqing 400715, China
e-mail: cshong@swu.edu.cn

sensors for the detection of Con A. In their work, ConA was binding to thiolated carbohydrate derivatives (D-mannose or D-glucose), which were immobilized onto screen-printed carbon electrodes (SPCEs) modified with gold nanoparticles. Because gold nanoparticles can enhance surface plasmon resonance response, Huang et al. reported dextran-capped gold nanoparticles based SPR sensor for ConA detection [9]. Generally, the development of these assay methods relied on employing the derivatives of mannose as recognition elements thereby suffering from tedious procedures for preparing derivatives of carbohydrate and low sensitivity. Hence, it is significant to explore a facile, simple, sensitive, and selective assay method for ConA.

Electrochemiluminescence, integrating the electrochemical and luminescent techniques, has become a powerful chemical sensing technique in recent years because of its advantages of simplicity, rapidity, sensitivity, controllability, and low background noise [12]. ECL techniques were widely applied in pharmaceutical analysis, environmental pollutant determination, and immunoassays [13]. As a common ECL reagent, luminol (5-amino-2, 3-dihydro-1,4- phthalazinedione) owns the merits of low oxidation potential, inexpensive reagent consumption, and high emission yields. However, as the most widely used co-reactant for luminol's electrochemiluminescence, H_2O_2, is not only unstable at room temperature but also difficult to be labeled [14]. Furthermore, H_2O_2 is a bit poisonous to some biomolecules. These flaws may be the factors that limit the application of luminol–H_2O_2 ECL system in the detection of biomolecules. Fortunately, H_2O_2 is the product of some enzymes catalyzed reactions. For instance, it is well known that glucose will be oxidized to gluconic acid and meanwhile generate H_2O_2 by the catalytical action of GOx [15]:

$$\text{glucose} + O_2 \xrightarrow{\text{GOx}} \text{gluconic acid} + H_2O_2$$

What's more, glucose is stable at the experimental conditions. Therefore, if the co-reactant, H_2O_2, is generated in situ from the glucose, and sequentially engages in ECL reaction, the shortage of instability of H_2O_2 directly as a co-reactant will be overcome, thereby improving the sensitivity and stability of the biosensor.

As a novel one-atom-thick two-dimensional graphitic carbon system, graphene and its derivatives possess remarkable physicochemical properties, such as high surface area (calculated value, 2630 m^2/g), strong mechanical strength, excellently optical and electronic properties, and facile surface modification [9, 16]. These properties make graphene and its derivatives good supports for immobilizing biomolecules and other nanomaterial. Owing to the above-mentioned excellent properties, graphene has caused extensive concern in developing biosensors [17–20].

In this work, we used the ECL detection method to develop an ultrasensitive biosensor for ConA detection based on biospecific interactions between carbohydrate residues of GOx and ConA. First, we synthesized amido functionalized graphene via reducing graphene oxide with poly(ethylenimine) (PEI), noted as PEI-rGO. This nanomaterial was modified on glassy carbon electrode (GCE) to assemble hollow gold nanoparticles (HAuNPs) by the interaction between Au and $–NH_2$. The HAuNPs showed an excellent electroactivity to luminol oxidization and, therefore, could greatly amplify the ECL signal of luminol, offering a highly sensitive ECL biosensor [21]. Then GOx was assembled onto this modified electrode through physical adsorption and covalent binding interactions between HAuNPs and $–NH_2$ in GOx to recognize ConA for ConA detection. Also, GOx could catalyze glucose to produce H_2O_2 in situ to strongly improve the ECL signal of luminol. After ConA was immobilized on the electrode, the intensity of ECL signal decreased, and was directly proportional to the logarithm of ConA concentration. The mechanism is briefly illustrated in Scheme 1.

Experimental

Reagents

Glucose oxidase (GOx), bovine serum albumin (BSA, 96 %–99 %), luminol (5-amino-2, 3-dihydro-1,4-phthalazinedione), concanavalin A (ConA, from *CanaValia ensiformis* jack bean), and phytohemagglutinin (PHA) were purchased from Sigma Chemical Co. (St. Louis, MO, USA). Hydrogen tetrachloroaurate ($HAuCl_4 \cdot 4H_2O$) was obtained from Shanghai Chemical Reagent Co. (Shanghai, China). Alpha fetoprotein (AFP) was purchased from Biocell (Zhengzhou, China). Carbohydrate antigen 15-3 (CA15-3) was received from Biocell Co. (Zhengzhou, China). Poly(ethylenimine) (PEI, 50 %) was purchased from Sigma Chemical Co. (St. Louis, MO, USA). Graphene oxide (GO) was purchased from Nanking Xianfeng Nano Co. (Nanking, China). Phosphate-buffered saline (PBS) solutions containing 0.10 M KCl, 0.10 mM Ca^{2+} and 0.10 mM Mg^{2+} were prepared with 0.10 M H_3PO_4, adjusted pH with concentrated NaOH solution. Ferricyanide solutions containing 5.0 mM $K_3Fe(CN)_6$ and 5.0 mM $K_4Fe(CN)_6$ were used as a redox reporter. A stock ConA solution (1.0 mg/mL) was prepared in PBS (0.075 M, pH 7.4) containing 0.10 mM Ca^{2+} and 0.10 mM Mg^{2+} and stored at 4 °C. Herein, Ca^{2+} and Mn^{2+} were necessary to activate ConA conformation [1]. A stock solution of luminol (0.010 M) was prepared by dissolving luminol in 0.10 M NaOH solution and was kept at 4 °C when not in use. For control experiment, solid gold nanoparticles (SAuNPs) were synthesized according to a method described in literature [22]. All other chemicals were of

analytical grade and were used as received. Deionized water was used throughout this study.

Apparatus and measurement

ECL emission was measured using a model MPI-A electrochemiluminescence analyzer (Xi'an Remax Electronic Science & Technology Co. Ltd., China), equipped with a photomultiplier tube (PMT) with its voltage set at 800 V. The ECL emission was recorded at the biosensor in an ECL detector cell containing 3 mL PBS with an appropriate concentration of luminol and glucose. The potential was set 0.2–0.8 V (vs. Ag/AgCl) at a scan rate of 0.3 V/s in the detection process. Cyclic voltammetry (CV) was performed with a CHI 600D electrochemical work station (Shanghai CH Instruments Co., China). Absorption spectra were recorded by a UV-2450 UV-VIS Spectrophotometer from Shimadzu Corp. (Tokyo, Japan). The conventional three-electrode system with a modified glassy carbon electrode as working electrode, a saturated calomel electrode (SCE) or Ag/AgCl (saturated KCl) as reference electrode, and a platinum wire as counter electrode was used in the detection process. Scanning electron microscopy (SEM) was conducted using a Hitachi scanning electron microscope (Hitachi S-4800; Japan). The Fourier-transform infrared spectroscopy (FT-IR) was recorded on a Nexus 670 FT-IR spectrophotometer (Nicolet Instruments, Tokyo) using KBr pellets. All of the above experiments were carried out at room temperature.

The synthesis of HAuNPs and PEI-rGO nanosheet

HAuNPs was prepared according to the methods in reference [23] with minor modification. First, 200 μL 0.10 M trisodium citrate solution was added to 50 mL double distilled water with rapid magnetic stirring under the nitrogen (N_2) atmosphere to get rid of dissolved oxygen. Then, 200 μL of a freshly prepared $NaBH_4$ (1.0 M) and 50 μL $CoCl_2$ (0.50 M) solution were added, respectively. When the color of the solution changed from pale pink to gray, 25 μL 1 % (w/w) $HAuCl_4$ solution was slowly added in drops six times, namely 150 μL 1 % $HAuCl_4$ was needed in total. The color of the solution changed from dark brown to a deep blue. The remaining cobalt nanoparticles were gradually oxidized under ambient conditions and left from the solution with rapid stirring for 30 min, leaving HAuNPs. The HAuNPs were collected and washed by centrifugation with double distilled water, and then dispersed in 2 mL double distilled water for further use.

PEI-rGO nanosheets were prepared according to a previously described method [24] with a little modification. Briefly, 5.0 mL dispersion of exfoliated GO sheets (1.0 ng/mL) was mixed with PEI (3 %, 0.50 mL) and heated under reflux in an oil bath at 135 °C for about 3 h. Herein, the PEI not only served as a reductant to reduce GO sheets but also provided the abundant amido to prevent the aggregates of graphene and combine HAuNPs. The obtained black PEI-rGO dispersion was washed by centrifugation with double distilled water to remove redundant PEI and then redispersed in 2.0 mL water.

Biosensor preparation

The glassy carbon electrode (Φ=4 mm) was successively polished using 0.3 and 0.05 μm alumina slurry, and then washed ultrasonically in ethanol and water for 3 min, respectively. Eight μL PEI-rGO suspensions were cast onto a pretreated GCE surface and dried at room temperature. Next, this modified electrode was incubated in hollow gold colloidal solution and left overnight to adsorb HAuNPs. The modified electrode was immersed in GOx solution for 12 h. Finally, the electrode was incubated in different concentrations of ConA solution for 1 h for biospecific reaction before each measurement. The modified electrode was thoroughly cleaned with PBS (pH 7.4) to remove the non-chemadsorbed species after every modification step. The configuration of the biosensors is presented in Scheme 1. Inset A shows the SEM image of HAuNPs. A rough surface and a relatively dark center were observed. The dark place was caused by nonconductivity of the hollow structure inside the gold nanoparticles.

Results and discussion

Characterization of PEI-rGO

Supplementary Figure 1A (see Electronic Supplementary Material, ESM) shows the UV-vis absorption spectra of GO and PEI-rGO water dispersions. In the spectrum of GO (curve a), two characteristic absorption peaks were observed. The peak at 228 nm was ascribed to the $\pi \rightarrow \pi^*$ transition of C=C, and the shoulder at about 307 nm corresponding to the $n \rightarrow \pi^*$ transition of C=O [25]. For PEI-rGO (curve b), the absorption peak of the $\pi \rightarrow \pi^*$ transition of C=C red-shifted to 264 nm, suggesting that the electronic conjugation within the graphene was restored after the reduction by PEI. This result is consistent with the absorption of aqueous stable graphene dispersion.

FT-IR spectroscopy is considered to be an important tool for characterizing functional groups. Supplementary Figure S1B (see ESM) presents the FT-IR spectra of the samples. As seen in curve a, the peak at 1053 arose from epoxy (–O-) groups. The peak at 1393 was assigned to a C–O vibrational mode. The peak at 1632 cm^{-1} corresponded with the vibrational mode of the ketone (–C=O) groups. The broad peak at 3426 cm^{-1} denoted C–OH stretching [26]. These oxygen containing groups were typical functional groups in

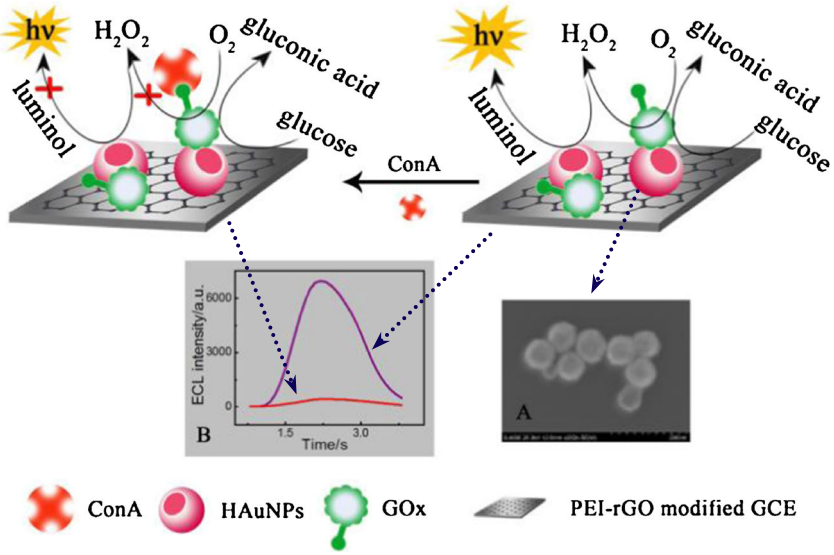

Scheme 1 Schematic representation of the configuration and detection mechanism of the biosensor. Inset **(A)** is the SEM image of HAuNPs. Inset **(B)** is the diagram of the change of ECL signal

GO. After reduced by PEI, the characteristic peaks of ketone groups disappeared, suggesting that GO had been successfully reduced. New peaks at 1551 and 1647 attributed to bending vibration of N-H band was noticed, indicating that PEI-rGO have been functionalized with amido [27].

Characterization of the biosensors fabrication process

Cyclic voltammetry (CV) was used to evaluate the assembly process of the modified electrode. The cyclic voltammograms (CVs) of different modified electrodes were obtained with $Fe(CN)_6^{4-/3-}$ as an electroactive probe and the results are presented in Fig. 1. As seen, a couple of quasi-reversible redox peaks of the probes was noticed in the bare electrode (curve a). When the electrode was modified with PEI-rGO, an increase in the peak current was observed (curve b). This was due to the fact that the electron active PEI-rGO could not only accelerate the electron transfer between the $Fe(CN)_6^{4-/3-}$ and

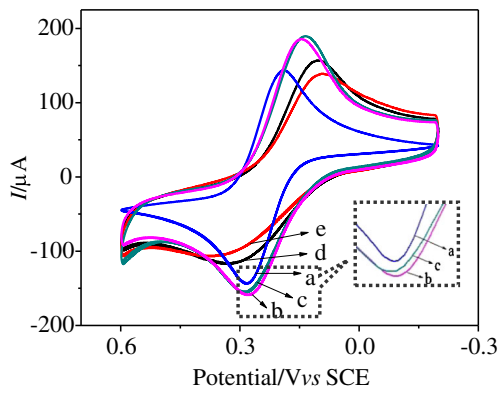

Fig. 1 CVs of **(a)** bare GCE, **(b)** PEI-rGO/GCE, **(c)** HAuNPs/PEI-rGO/GCE, **(d)** GOx/HAuNPs/PEI-rGO/GCE, and **(e)** ConA/GOx/HAuNPs/PEI-rGO/GCE in 5.0 mM $K_3[Fe(CN)_6]/K_4[Fe(CN)_6]$ (1:1). Scan rate: 50 mV/s

the electrode but also increase the interface area [18]. For the HAuNPs/PEI-rGO/GCE, there was still a strong current response (curve c). When the electrode was successively incubated in GOx (curve d) and ConA (curve e) solution, the peak currents declined at corresponding CVs, which was ascribed to the nonconductive properties of GOx and ConA. The CV study proved that the biosensor has been successfully prepared.

SEM was used to observe the interfacial changes of the electrode surface during the fabrication process. Typical SEM images of different materials modified films are shown in Fig. 2. PEI-rGO showed a typical wrinkle morphology and silk-like shape with a very thin layer (Fig. 2a). With the adsorption of HAuNPs on the PEI-rGO, hollow nanospheres were obviously observed (Fig. 2b). When coated with GOx and ConA (Fig. 2c), the corresponding SEM image became darker because of the non-conductive GOx and ConA.

Optimization of analytical conditions

The important factors including luminol concentration, glucose concentration, and scan rate, which affect the performance of the prepared biosensors, had been discussed. Supplementary Figure S2A (see ESM) shows the influence of luminol concentration on ECL response. As can be seen, when the concentration of luminol increased in the range of 0.050–0.20 mM, a distinct increase in ECL intensity was noticed. However, further increase of luminol concentration caused only a slight enhancement in ECL signal. Therefore 0.20 mM luminol was chosen for the quantitative analysis.

The concentration of glucose needs to be investigated because glucose can react with O_2 to generate H_2O_2 by the catalytic action of GOx, and H_2O_2 as a co-reactant of luminol can obviously enhance the ECL signal of luminol. The experimental results are shown in Supplementary Figure S2B (see

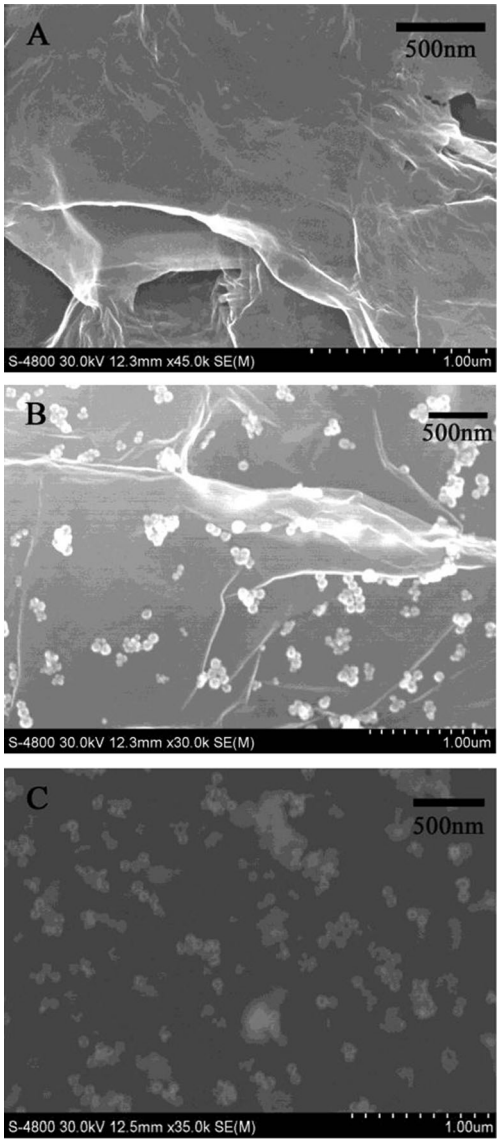

Fig. 2 SEM images of **(a)** PEI-rGO, **(b)** HAuNPs/PEI-rGO, and **(c)** ConA/GOx/HAuNPs/PEI-rGO modified films

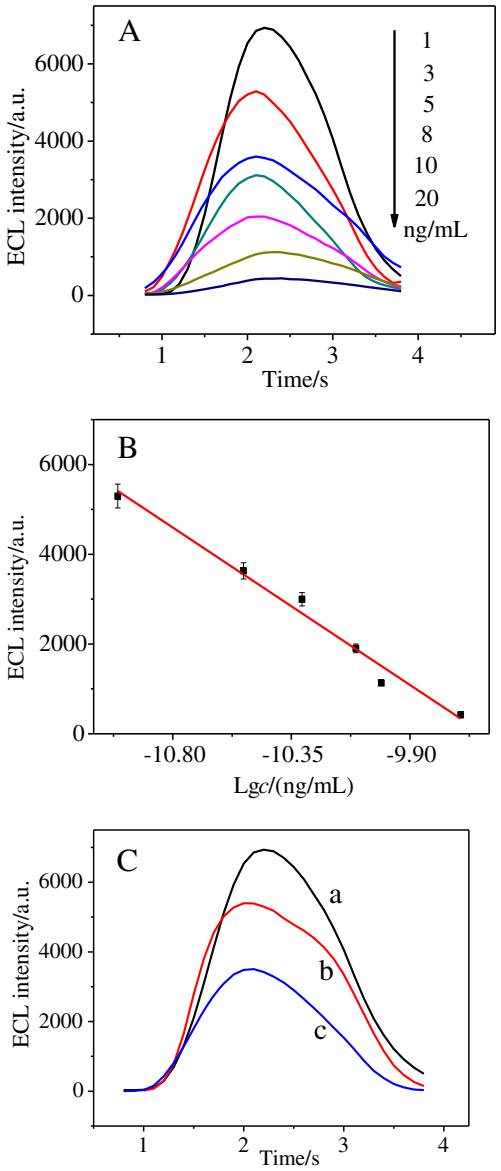

Fig. 3 **(a)** ECL response of the biosensor towards the ConA in 0.075 M PBS solution (pH 7.4) containing 0.20 mM luminol and 0.030 M glucose. Scan rate: 0.3 V/s. **(b)** The linear relationship between the ECL intensity and the ConA concentrations. Error bars were obtained from three times parallel experiments. **(c)** ECL responses of **(a)** GOx/HAuNPs/PEI-rGO/GCE, **(b)** GOx/SAuNPs/PEI-rGO/GCE, and **(c)** GOx/PEI-rGO/GCE

ESM). As seen, the ECL response gradually enhanced with the concentration of glucose in the range of 0.010–0.030 M. However, when the concentration of glucose exceeded 0.030 M, the ECL intensity increased slowly. Hence, 0.030 M was chosen as the optimal concentration of glucose in this experiment.

Supplementary Figure S2C (see ESM) presents the effect of scan rate on ECL signal. As seen, maximum ECL signal was achieved at 0.3 V/s. Therefore, 0.3 V/s was chosen for ECL analysis of ConA.

Quantitative analysis of ConA

Under the optimized experimental conditions, we explored the ECL response of the prepared biosensor towards different concentration of ConA, and the ECL responses were recorded under continuous scanning to obtain a relative steady ECL signal. As expected, the ECL signal decreased gradually with the increase in ConA concentration (Fig. 3a). The corresponding standard calibration curve of the ECL intensity versus logarithm of ConA concentration is shown in the Fig. 3b. Under the optimal conditions, the linear range for ConA was from 1.0 ng/mL to 20 ng/mL with a detection limit of 0.31 ng/mL (signal to noise ratio =3) and the limit of quantity of 0.93 ng/mL (signal to noise ratio =10). The linear equation was I=5408.9-3898.3 log$c$ (where I was the ECL intensity and c was the concentration of ConA), and the correlation

coefficient was 0.991. According to the linear equation, the prepared biosensors could be used to quantitatively detect ConA. Higher concentration can be detected after dilution using the prepared biosensors. Compared with the results of most previous reports, our prepared biosensors exhibited a high sensitivity and a low detection limit. A nearly 1000-fold improvement in detection limit was obtained. The details of a comparison between our method and reported methods are provided in Supplementary Table S1 (see ESM). Overall, the prepared biosensors in this work exhibited excellent performance. The reasons are described as follows. First, PEI-rGO nanosheets with large surface area as supporting matrix increased the loading amount of HAuNPs. Second, HAuNPs showed excellent electroactivity to luminol oxidization and, therefore, could greatly amplify the ECL signal of luminol [21]. Compared with SAuNPs, HAuNPs presented a rough surface and possessed a larger surface area. Third, the good electrocatalytic activity and conductivity of PEI-rGO and HAuNPs made them accelerate electron transfer between the electrode surface and the activity center of GOx. Moreover, it is also reported that gold nanoparticles have excellent catalytic performance to directly enhance the ECL intensity of luminol-H_2O_2 system. The effect of HAuNPs was demonstrated by a control experiment among GOx/PEI-rGO/GCE, GOx/SAuNPs/PEI-rGO/GCE, and GOx/HAuNPs/PEI-rGO/GCE. The results are shown in Fig. 3c. It is seen that the biosensor with HAuNPs (curve a) has the strongest ECL response compared with GOx/SAuNPs/PEI-rGO/GCE (curve b) and GOx/PEI-rGO/GCE (curve c). Most importantly, the recognition element GOx can catalyze glucose to generate the co-reactant of luminol in situ, which highly enhances the ECL signal.

Reproducibility, stability, and selectivity of ECL biosensors

The reproducibility (inter- and intra-assay) of the ECL biosensor was investigated. The intra-assay precision of the biosensor was evaluated by testing a biosensor with 10 ng/mL ConA for five replicate determinations in PBS under the optimized experimental conditions. The inter-assay precision was estimated at five different biosensors in the same batch. The relative standard deviation (RSD) of intra-assay and inter-assay were found to be 4.1 % and 4.8 %, respectively, indicating acceptable reproducibility.

When the 12 cyclic scans was carried out in the potential range from 0.2 to 0.8 V with a scan rate of 0.3 V/s, the ECL signal decreased slowly for the first four cycles, which may be attributed to the consumption of luminol. Then, the ECL signal kept nearly constant (Supplementary Figure S3 in ESM), which was due to the good stability of the electrode materials and in situ generated H_2O_2 for ECL signal enhancement, thereby counteracting the decrease in ECL signal. On the other hand, the storage stability of the prepared biosensor was also studied. When not in use, the electrode was suspended above 0.075 M phosphate buffer at 4 °C in a refrigerator. The ECL response to 10 ng/mL ConA was tested every 2 to 3 d; after 10 d, the ECL response decreased to about 9.3 % of its initial response, indicating an acceptable stability of the biosensor.

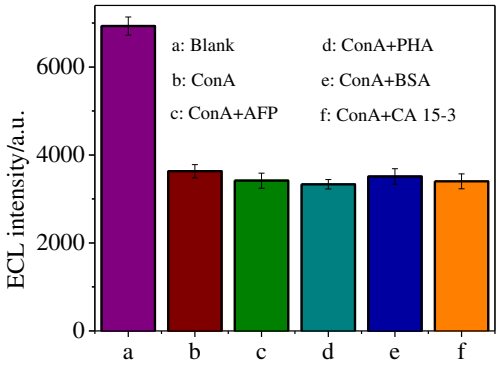

Fig. 4 ECL response of the biosensor incubated in **(a)** blank, **(b)** ConA (3 ng/mL), a mixture of ConA (3 ng/mL), and **(c)** AFP (20 ng/mL), **(d)** PHA (50 ng/mL), **(e)** BSA (1 %), **(f)** CA 15-3 (0.1 U/mL), respectively. Error bars were obtained from three times parallel experiments

To further study the selectivity of the biosensor, it was incubated in 3 ng/mL ConA containing different interfering agents such as AFP, BSA, CA 15-3, and PHA, respectively. The corresponding results were shown in Fig. 4. The interference caused by these substances could be neglected, indicating a good selectivity of the prepared biosensors for ConA.

Application of the biosensors

In order to examine the reliability and potential application of the prepared ECL biosensors, the recovery experiments of ConA were performed in PBS and four real samples including fetal bovine serum and three real human blood samples (diluted by PBS). Experimental results are presented in Supplementary Table S2 (in ESM). The recoveries (94.2 %–109 %) were acceptable, indicating that the prepared ECL biosensor was specific to ConA in biological fluids without observable interference.

Conclusion

In this work, an ECL biosensor for sensitive detection of ConA was developed using GOx as a recognition element and for signal enhancement by catalyzing glucose to in situ generate H_2O_2, the co-reactant of luminol. The proposal of in situ generating co-reactant of luminol overcame the shortage of instability of H_2O_2 directly as co-reactant, and thereby was propitious to improve the sensitivity and stability of the prepared biosensors. What's more, the combination PEI-rGO

nanosheets and HAuNPs could not only endow the biosensor high loading of GOx, but also accelerate the electron transfer because of their excellent electro-catalytic activity. The designed ECL biosensor exhibited excellent performance, such as high sensitivity, good stability, and selectivity for ConA detection. Moreover, compared with the method reported in Reference [9], the constructed ECL biosensor offered many other advantages, including simplicity of preparation and manipulation. Thus, this scheme for ConA detection may exhibit potential application.

Acknowledgments This work was financially supported by the NNSF of China (21075100, 21275119, 21105081), Ministry of Education of China (Project 708073), Research Fund for the Doctoral Program of Higher Education (RFDP) (20110182120010), Natural Science Foundation of Chongqing City (CSTC-2011BA7003, CSTC-2010BB4121), State Key Laboratory of Silkworm Genome Biology (sklsgb2013012), and the Fundamental Research Funds for the Central Universities (XDJK2013A008, XDJK2013A27), China.

References

1. Loaiza OA, Lamas-Ardisana PJ, Jubete E, Ochoteco E, Loinaz I, Cabañero G, García I, Penades S (2011) Nanostructured disposable impedimetric sensors as tools for specific biomolecular interactions: sensitive recognition of concanavalin A. Anal Chem 83:2987–2995
2. Bellapadrona G, Tesler AB, Grünstein D, Hossain LH, Kikkeri R, Seeberger PH, Vaskevich A, Rubinstein I (2012) Optimization of localized surface plasmon resonance transducers for studying carbohydrate-protein interactions. Anal Chem 84:232–240
3. Yonzon CR, Jeoung E, Zou S, Schatz GC, Mrksich M, Duyne RPV (2004) A comparative analysis of localized and propagating surface plasmon resonance sensors: the binding of concanavalin A to a monosaccharide functionalized self-assembled monolayer. J Am Chem Soc 126:12669–12676
4. Li WJ, Yuan R, Chai YQ (2010) Determination of glucose using pseudobienzyme channeling based on sugar–lectin biospecific interactions in a novel organic-inorganic composite matrix. J Phys Chem C 114:21397–21404
5. Zou L, Pang HL, Chan PH, Huang ZS, Gu LQ, Wong KY (2008) Trityl-derivatized carbohydrates immobilized on a polystyrene microplate. Carbohydr Res 343:2932–2938
6. Huang CC, Chen CT, Shiang YC, Lin ZH, Chang HT (2009) Synthesis of fluorescent carbohydrate-protected Au nanodots for detection of concanavalin A and escherichia coli. Anal Chem 81:875–882
7. Guo CX, Boullanger P, Jiang L, Liu T (2007) Highly sensitive gold nanoparticles biosensor chips modified with a self-assembled bilayer for detection of Con A. Biosens Bioelectron 22:1830–1834
8. Hone DC, Haines AH, Russell DA (2003) rapid, quantitative colorimetric detection of a lectin using mannose-stabilized gold nanoparticles. Langmuir 19:7141–7144
9. Huang CF, Yao GH, Liang RP, Qiu JD (2013) Graphene oxide and dextran capped gold nanoparticles based surface plasmon resonance sensor for sensitive detection of concanavalin A. Biosens Bioelectron 50:305–310
10. Hu F, Chen S, Wang C, Yuan R, Xiang Y, Wang C (2012) Multi-wall carbon nanotube-polyaniline biosensor based on lectin–carbohydrate affinity for ultrasensitive detection of Con A. Biosens Bioelectron 34: 202–207
11. Guo C, Boullanger P, Jiang L, Liu T (2008) One-step immobilization of alkanethiol/glycolipid vesicles onto gold electrode: amperometric detection of Concanavalin A. Colloids Surf, B 62:146–150
12. Xu S, Liu Y, Wang T, Li J (2011) Positive potential operation of a cathodic electrogenerated chemiluminescence immunosensor based on luminol and graphene for cancer biomarker detection. Anal Chem 83:3817–3823
13. Wang HJ, Yuan R, Chai YQ, Niu H, Cao YL, Liu H (2012) Bienzyme synergetic catalysis to *in situ* generate coreactant of peroxydisulfate solution for ultrasensitive electrochemiluminescence immunoassay. Biosens Bioelectron 37:6–10
14. Cao YL, Yuan R, Chai YQ, Mao L, Niu H, Liu HJ, Zhuo Y (2012) Ultrasensitive luminol electrochemiluminescence for protein detection based on *in situ* generated hydrogen peroxide as coreactant with glucose oxidase anchored AuNPs@MWCNTs labeling. Biosens Bioelectron 31:305–309
15. Jiang XY, Chai YQ, Wang H, Yuan R (2014) Electrochemiluminescence of luminol enhanced by the synergetic catalysis of hemin and silver nanoparticles for sensitive protein detection. Biosens Bioelectron 54:20–29
16. Chen D, Feng H, Li J (2012) Graphene oxide: preparation, functionalization, and electrochemical applications. Chem Rev 112: 6027–6053
17. Valentini F, Carbone M, Palleschi G (2013) Graphene oxide nanoribbons (GNO), reduced graphene nanoribbons (GNR), and multi-layers of oxidized graphene functionalized with ionic liquids (GO–IL) for assembly of miniaturized electrochemical devices. Anal Bioanal Chem 405:3449–3474
18. Zhang Y, Dai WJ, Liu F, Li L, Li M, Ge SG, Yan M, Yu JH (2013) Ultrasensitive electrochemiluminescent immunosensor based on dual signal amplification strategy of gold nanoparticles-dotted graphene composites and CdTe quantum dots coated silica nanoparticles. Anal Bioanal Chem 405:4921–4929
19. Wang HB, Ou LJ, Huang KJ, Wen XG, Wang LL, Liu YM (2013) A sensitive biosensing strategy for DNA detection based on graphene oxide and T7 exonuclease assisted target recycling amplification. J Chem 91:1266–1271
20. Szunerits S, Maalouli N, Wijaya E, Vilcot JP, Boukherroub R (2013) Recent advances in the development of graphene-based surface plasmon resonance (SPR) interfaces. Anal Bioanal Chem 405:1435–1443
21. Xu SJ, Liu Y, Wang TH, Li JH (2010) Highly sensitive electrogenerated chemiluminescence biosensor in profiling protein kinase activity and inhibition using gold nanoparticle as signal transduction probes. Anal Chem 82:9566–9572
22. Frens G (1973) Controlled nucleation for the regulation of the particle size in monodisperse gold suspensions. Nat Phys Sci 241:20–22
23. Schwartzberg AM, Oshiro TY, Zhang JZ, Huser T, Talley CE (2006) Improving nanoprobes using surface-enhanced raman scattering from 30-nm hollow gold particles. Anal Chem 78:4732–4736
24. Cao LY, Liu YL, Zhang BH, Lu LH (2010) *In situ* controllable growth of prussian blue nanocubes on reduced graphene oxide: facile synthesis and their application as enhanced annoelectrocatalyst for H_2O_2 reduction. ACS Appl Mat Interfaces 2:2339–2346
25. Li LL, Liu KP, Yang GH, Wang CM, Zhang JR, Zhu JJ (2011) Fabrication of graphene–quantum dots composites for sensitive electrogenerated chemiluminescence Immunosensing. Adv Funct Mater 21:869–878
26. Lee DW, De Los Santos LV, Seo JW, Leon Felix L, Bustamante DA, Cole JM, Barnes CHW (2010) The structure of graphite oxide: investigation of its surface chemical groups. J Phys Chem B 114: 5723–5728
27. Jiang L, Gao L (2003) Modified carbon nanotubes: an effective way to selective attachment of gold nanoparticles. Carbon 41:2923–2929